Bulgarian Chemical Communications, Volume 55, Issue 3 (pp. 227-233) 2023 DOI: 10.34049/bcc.55.3.ICNTC01

The reactivity properties of platinum-containing anticancer drugs

S. Aydogdu, M. Evirgen, A. Hatipoglu*

Faculty of Arts and Sciences, Department of Chemistry, Yildiz Technical University,34220 Istanbul, Turkey

Accepted: August 07, 2023

Cisplatin has been an important platinum-containing anticancer drug for years. Toxic effects of cisplatin and the resistance of tumor cells against treatment lead to new studies about finding new Pt- containing anticancer drugs. In this study, the electronic properties and reactivity indices of cisplatin and its clinically accepted derivatives carboplatin, oxaliplatin, nedaplatin, lobaplatin, and heptaplatin were calculated by density functional theory (DFT). These properties of drugs have been calculated in both vacuum and aqueous medium. The reactivity of the molecules is explained with the global reactivity indices. Local reactivity indices were used to examine the reaction of the hydrolyzed nedaplatin complex with the amino acid cysteine. In anticancer drugs containing Pt, the platinum atom is an important reaction site for anticancer mechanisms.

Keywords*:* anticancer, cisplatin derivatives, DFT, aqueous medium, reactivity indices

INTRODUCTION

In the late 1960s, a new era began in antineoplastic drugs with the discovery of cisplatin [1, 2]. Understanding the anticancer properties of cisplatin made it the pioneer of metal-based anticancer drugs used from the past to the present [3]. However, cisplatin lacks tumor tissue selectivity and makes target cells resistant to cisplatin over time [4]. Therefore, scientists have synthesized new cisplatin analogs such as carboplatin, oxaliplatin, nedaplatin, lobaplatin, and heptaplatin. These platinum-based chemotherapeutic drugs are the most widely used ones in the treatment of different cancer diseases [5]. Also, scientists have made progress in the research of the different metal-based anticancer drugs in recent years [6, 7].

Cisplatin is used in the treatment of many cancers, especially testicular and ovarian, also colon, stomach, breast, prostate, and small cell and non-small cell lung [8]. The mechanism of action depends on the platinization of DNA bases. In this process, hydrolysis of the drug is an important step that makes it easier to reach the drug to DNA. In addition, hydrolysis of the drug is essential to activate the drug [2, 9]. Pt-S and Pt-N bonds were found in the crystal structure of the drug's addicted product. This means that the platinum atom of the drug binds to amino acids of DNA from their S or N atoms [9]. The resultant structural form suppresses the efficient replication of tumor DNA and as a result of this anticancer effect the tumor cell dies [2].

Despite the great benefits of platinum chemotherapeutics, they have also various side effects such as nephrotoxicity and negative effects on the liver [8]. In addition to the toxicities of the drug, long-term use of cisplatin causes cisplatin resistance. The ability of cross-linking feature of cisplatin provides that cisplatin cross-links to the DNA of the target cell and prevents its dividing [10]. Thus, the formation of resistance is the binding of platinum to DNA and the main cytotoxic mechanism that occurs after cisplatin enters tumor cells [11]. To elucidate the mechanism of such disadvantages and side effects, studies have been carried out to examine many properties of cisplatin such as its electronic and molecular structure [4, 12].

In one of the studies, the effects of catalpol (CAT), a bioactive component, on cisplatin-induced nephrotoxicity and antitumor activity were investigated. As a result of the research, it has been observed that CAT can reverse drug resistance without compromising the antitumor properties of cisplatin. This shows that CAT has positive effects against cisplatin-induced kidney damage by reversing drug resistance *via* the mitochondrial-dependent pathway without affecting the anticancer activity of cisplatin [13]. Another study showed that the anticancer effect of cisplatin was strengthened by nano curcumin. So, they achieved a significant reduction in ovarian tumor volume and weight with cisplatin and nano curcumin administration [14]. A study used nanosheets like Al-doped BN and Ga-doped BN towards cisplatin to understand the adsorption behavior of cisplatin [15]. They achieved higher HOMO energies and lower LUMO energies after the adsorption of cisplatin on the AIBN and GaBN nanosheets.

* To whom all correspondence should be sent:
E-mail: hatiparzu@yahoo.com

The reduction of the energy gap increases the conduction electron population which is important for the drug delivery system. As a result, nanosheets showed high adsorption behavior with small adsorption distances and large variations of the energy gap, especially AIBN. So, AIBN and GaBN nanosheets are promising candidates as drug delivery vehicles for cisplatin [15]. The experimental techniques are expensive to conduct and bring some problems to clinical trials such as losing the activity of a drug candidate before *in vivo* test. So, computational modeling studies are important to get information about molecules and to gain insight into their properties before expensive experimental periods [1].

Density functional theory (DFT) which is the most preferred quantum-mechanical method in recent years, provides important information about the physicochemical properties of compounds. Also, it is known that physicochemical properties are related to the biological activity of compounds [16]. DFT aims to understand the electronic structure and molecular dynamics of the molecules.

In this study, the electronic and physicochemical properties of cisplatin and its derivatives such as carboplatin, oxaliplatin, nedaplatin, lobaplatin, and heptaplatin were investigated. The calculations of the relevant molecules were carried out with the DFT method. The HOMO-LUMO energies, global and local reactivity indices, and thermochemical parameters were calculated in both vacuum and aqueous medium. In addition, the reaction of hydrolyzed nedaplatin complex with cysteine amino acid of DNA was explained by local reactivity indices.

COMPUTATIONAL METHODS

All geometric and electronic calculations were performed with the DFT method within Gaussian 09W software [17]. DFT calculations were carried out by using the three-parameter Becke-Lee-Yang-Parr (B3LYP) exchange-correlation functional with LanL2DZ basis set. Frequency analysis of the molecular structure as a global minimum was performed and all frequency values are positive. Frontier molecular orbitals (FMO), molecular electrostatic potential (MEP) surfaces, and structural visualizations of all molecules were prepared by using Gaussview 5.0 [18].

Global and local reactivity indices were also calculated for the studied molecules. Solvent effects were computed by using conductor-like polarizable continuum model (CPCM) as the solvation model. In this study solvent was water with a dielectric constant value of ε=78.355 [19].

Reactivity indices calculation

Reactivity indices are based on the perturbation of one chemical attacking another chemical species. These perturbations are related to the changing number of electrons or changing of an external potential. Global reactivity indices are related to changing of electrons. The variation of the boundary electron densities is defined by the local indices proposed by Fukui. Local indices give information about the reactivity of a particular region of the molecule [20, 21].

The global reactivity indices are calculated with the following Eq. (1-4). In these equations, E_{HOMO} and E_{LUMO} are the energy of the highest occupied molecular orbital and the lowest unoccupied molecular orbital, respectively. The hardness (η) is calculated by using Koopmans'theorem. [22].

$$\eta = \frac{(E_{LUMO} - E_{HOMO})}{2} \quad (1)$$

The global softness (S) is defined as inverse of the chemical hardness.

$$S = \frac{1}{2\eta} \quad (2)$$

Electronegativity (X), which is the negative of chemical potential (μ), is calculated with HOMO and LUMO energies. The electrophilic index depends on the values of chemical potential and hardness values.

$$X = -\mu = \left(\frac{-E_{HOMO} - E_{LUMO}}{2}\right) \quad (3)$$

$$\omega = \frac{\mu^2}{2\eta} = \frac{X^2}{2\eta} \quad (4)$$

The fukui indices can be calculated by Eqs. (5-7). In these equations, $p_{N0,}$ p_{N+1} and p_{N-1} represent the electronic population on an atom for the neutral, cation and anion systems, respectively. And $f^{+}_{(r)}$, $f^{-}_{(r)}$, $f^{0}_{(r)}$ are fukui indices for the nucleophilic attack, electrophilic attack, and radicalic attack, respectively [21, 23].

$$f^{+}_{(r)} = p_{N+1}(r) - p_N(r), \quad (5)$$

$$f^{-}_{(r)} = p_N(r) - p_{N-1}(r), \quad (6)$$

$$f^{0}_{(r)} = \frac{p_{N+1}(r) - p_{N-1}(r)}{2} = \frac{f^{+}_{(r)} - f^{-}_{(r)}}{2}, \quad (7)$$

RESULTS AND DISCUSSION

Ground state geometries and global reactivity indices

The molecular structures and the optimized structures of the studied molecules are given in Fig S1 and Fig. 1. The optimized geometrical parameters

and IR data of cisplatin are based on experimentally obtained results [24, 25]. The geometric parameters for other studied Pt- containing anticancer drugs are given in Table 1. The bond lengths of Pt-O and Pt-N are found to be 2.0 and 2.1 Å, respectively, for carboplatin, oxaliplatin, nedaplatin, lobaplatin, and heptaplatin. The approximate dihedral angle value of the five molecules is 0.51°. As also demonstrated in Fig 1, square planar geometric orientation is obtained for all studied molecules.

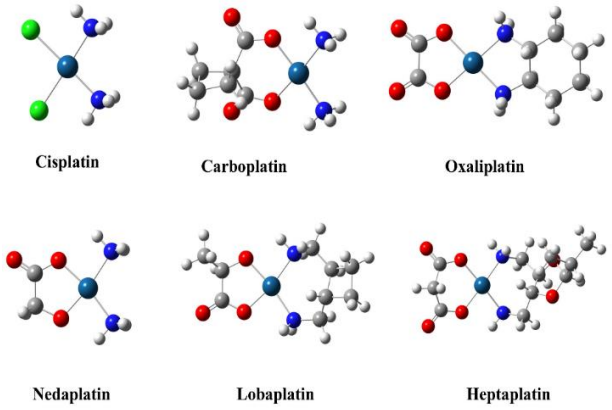

Figure 1. Optimized structures of cisplatin and derivatives.

Anticancer molecules containing Pt have different reactivity and stability due to their structures. In this study, global reactivity indices such as chemical hardness (η), global softness (S), electronegativity (X), and electrophilic index (ω) are calculated for vacuum (vac) and aqueous (aq) medium and they are listed in Table 2. The reactivity and stability of molecules can be interpreted by global reactivity indices. The higher hardness value indicated higher stability and lower reactivity because of the bigger energy gap between frontier orbitals. Softness is the inverse of hardness. As seen in Table 2, carboplatin and heptaplatin have the highest hardness values of 2.55 and 2.54 eV, respectively.

The hardness value of heptaplatin is close to that of carboplatin. These two molecules are more stable and less reactive than others. On the other hand, cisplatin has the highest softness value which is 0.23 eV and this makes cisplatin the most reactive molecule compared to others. This result is also in accordance with Alberto *et al*. study [2, 26].

The reactivity order of the molecules is: cisplatin > oxaliplatin > nedaplatin > lobaplatin > heptaplatin > carpoplatin. The acids must be more electronegative than the bases [27]. The highest electronegativity value has cisplatin with 4.09 eV, so cisplatin is the most acidic molecule.

Table 1. Calculated bond lengths, r and bond angles, a values of molecules

	Carboplatin	Oxaliplatin	Nedaplatin	Lobaplatin	Heptaplatin
r (Å)					
Pt-O	2.0	2.0	2.0	2.0	2.0
Pt-N	2.1	2.1	2.1	2.1	2.1
a (^{0})					
N-Pt-N	105.6	83.3	106.8	107.3	102.1
O-Pt-O	96.6	83.4	86.8	86.1	98.8

Table 2. Electronic properties (eV) of molecules

	Cisplatin		Carboplatin		Oxaliplatin		Nedaplatin		Lobaplatin		Heptaplatin	
	vac	aq	vac	aq	vac	aq	vac	aq	vac	aq	vac	aq
E_{HOMO}	-6.27	-6.49	-6.39	-6.40	-5.83	-6.44	-5.40	-5.62	-5.18	-5.55	-6.39	-6.46
E_{LUMO}	-1.90	-1.85	-1.28	-1.01	-1.06	-1.75	-0.66	-0.63	-0.38	-0.53	-1.30	-1.11
ΔE	4.37	4.65	5.11	5.39	4.77	4.69	4.74	4.99	4.80	5.02	5.08	5.35
X	4.09	4.17	3.84	3.70	3.44	4.09	3.03	3.12	2.78	3.04	3.85	3.79
η	2.18	2.32	2.55	2.70	2.39	2.35	2.37	2.50	2.40	2.51	2.54	2.68
ω	3.82	3.74	2.88	2.54	2.48	3.57	1.93	1.95	1.61	1.84	2.91	2.68
S	0.23	0.22	0.20	0.19	0.21	0.21	0.21	0.20	0.21	0.20	0.20	0.19

Lobaplatin is a basic molecule with the lowest electronegativity value of 2.78 eV. All of the molecules have electrophilic index values greater than 1.5 eV, which means that they are all strong electrophiles [28]. The chemical potential is negative. The electrophilic index contains information about electron transfer and it shows similar trends with chemical potential [29].

Frontier molecular orbitals

Frontier molecular orbitals (FMOs) are the electron distribution representations of HOMO and LUMO. They provide very important information such as electronic properties, kinetic stability, and chemical reactivity of molecules [30]. Frontier molecular orbitals of the studied molecules are given in Fig. 2. As seen in Fig 2 HOMO is located on the Pt atom, and chloride substitutions for cisplatin. In contrast to cisplatin results, HOMO of other drugs is located at the central Pt atom and butane dicarboxylate, glycolate, oxalate, 3-methyl butane-2-one, and pentane-2,4-dione for carboplatin, oxaliplatin, nedaplatin, lobaplatin, and heptaplatin respectively. LUMO of the molecules is distributed through the molecules except for oxaliplatin, lobaplatin, and heptaplatin. Electron distribution of LUMO for these molecules is mainly on the glycolate, 3-methyl butane-2-one, and pentane-2,4-dione parts of the molecules.

It is understood from Table 1 that HOMO energies decreased for all molecules in aqueous medium than in vacuum. On the other hand, LUMO energies did not decrease for all such as oxaliplatin and lobaplatin. However, the energy gap between HOMO and LUMO decreased only for oxaliplatin in aqueous medium than vacuum. Accordingly, unlike the others, oxaliplatin is more photochemically reactive in an aqueous medium than in vacuum.

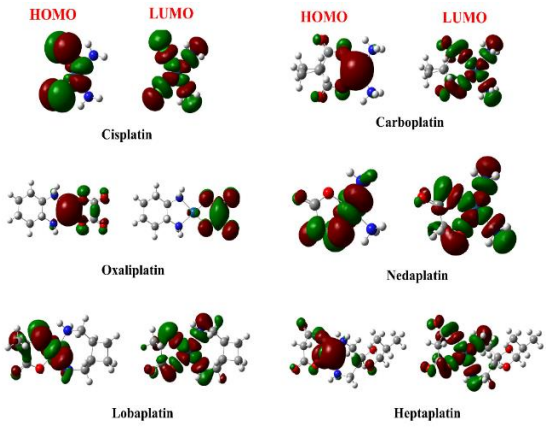

Figure 2. Frontier molecular orbitals of cisplatin derivatives

Molecular electrostatic potential (MEP)

The molecular electrostatic potential (MEP) surface is a three-dimensional visualized representation of the charge distributions of molecules on the electron density surface. MEP surfaces help to predict the shape, size, and reactive sides of molecules. The color identification of electrostatic potential is in the range of red and blue. The red depicts negative regions and they are related to an electrophilic attack whereas blue depicts positive regions and they are related to the nucleophilic attack. Electrostatic potential increases from red to blue [31]. MEP surfaces of studied molecules are illustrated in Fig. 3.

The positively charged regions shown in blue are mainly over the amine groups of all molecules. The negative charge distribution of the molecules is on carbonyl groups and oxygen, except for cisplatin. In cisplatin, it is on the chloride atoms. These blue regions have high electron abundance and an electrophilic attack occurs most likely from this side of the molecules. Pt atoms in these MEP surfaces are at the central place of the boundary between the negatively and positively charged areas for all molecules.

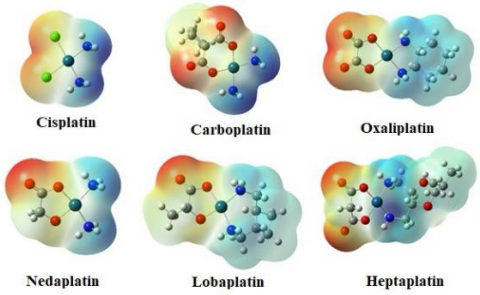

Figure 3. MEP surfaces of cisplatin derivatives

Reaction of nedaplatin with cysteine amino acid

Fukui indices are the most important local properties used in determining the reactivity of different regions of a molecule. In this part of the study, the reaction of cysteine amino acid with anticancer drugs containing Pt was investigated by local fukui indices. For this, nedaplatin was chosen as the model molecule. These types of reactions are necessary to understand the anticancer activities of Pt-containing anticancer drugs with DNA.

It is known from the literature that the Pt atom has a soft character, so it can interact with the S atom in the cysteine amino acid of DNA [32, 33]. Fukui indices results of nedaplatin in aqueous medium are given in Table 3.

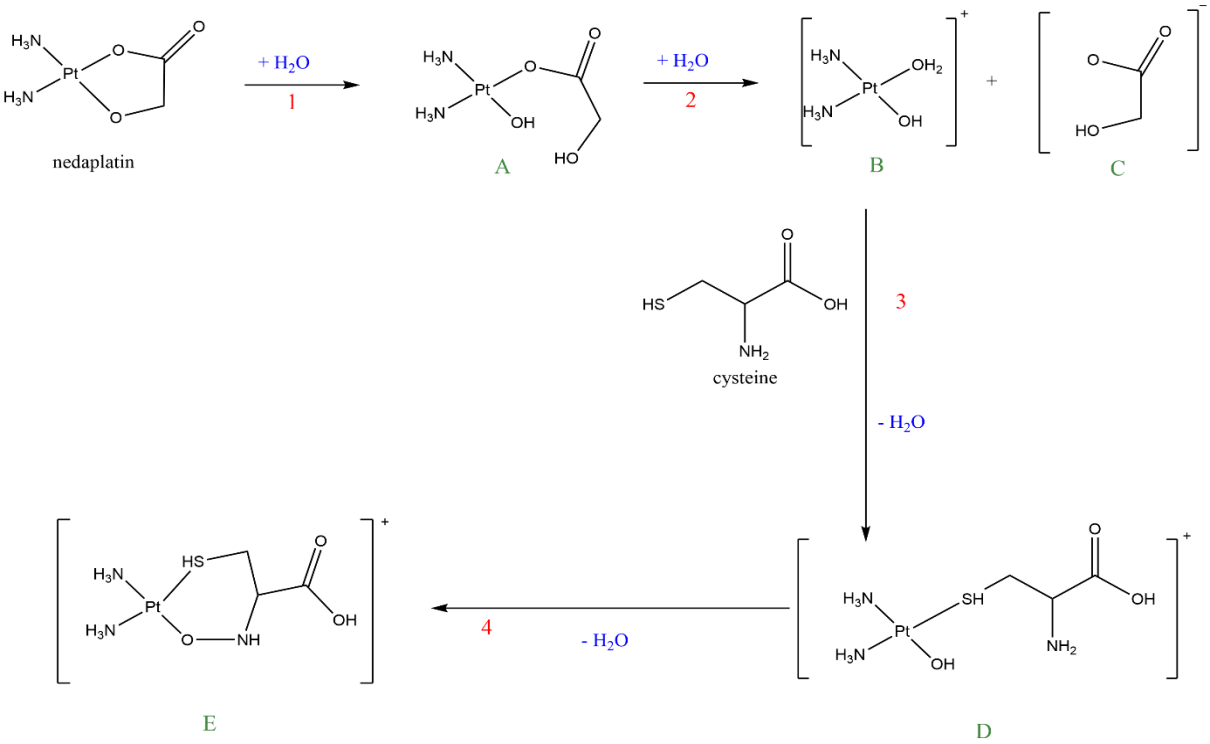

Scheme 1. The predicted reaction mechanism of nedaplatin

Table 3. Fukui indices of nedaplatin and cysteine

		Nedaplatin					Cysteine		
		f+	f-	f0			f+	f-	f0
1	Pt	0.472	0.422	0.447	1	N	0.015	0.188	0.102
2	O	0.037	0.186	0.112	3	C	0.040	-0.028	0.006
3	O	0.015	0.017	0.016	5	C	-0.008	0.004	-0.002
4	C	0.056	0.047	0.052	6	C	0.262	0.040	0.151
5	O	0.044	0.043	0.044	9	S	0.074	0.313	0.194
12	N	0.042	0.012	0.027	10	O	0.209	0.073	0.141
13	N	0.031	0.013	0.022	13	O	0.094	0.029	0.062
14	C	0.033	-0.004	0.015					

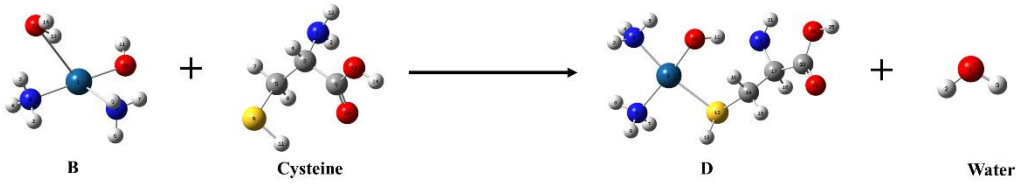

Figure 4. Optimized geometries for the reaction path 3.

The greater the value of the fukui indices of an atom in the molecule, the higher its reactivity. Therefore, these values are listed in the table. It is demonstrated in Table 3 that the Pt atom site is a suitable part for nucleophilic attack of amino acids and this result is compatible with the literature [32, 33]. Fukui indices of other studied molecules are given in the Supplementary material. Similar to Zimmermann *et al*. study Pt atom sites of other drugs are also found as the most suitable part for DNA reactions [33].The reaction mechanism of nedaplatin with cysteine is given in Scheme 1. As seen from Scheme 1 the reaction mechanism begins with the hydrolyzing of nedaplatin. It is accepted that hydrolysis of nedaplatin is essential to react with DNA [26]. Thus, hydrolysis of nedaplatin occurs first in the mechanism, and then it binds to the amino acid portion of the DNA.

It is understood from Scheme 1 that hydrolysis of nedaplatin is occurred with two executive steps, paths 1 and 2. As nedaplatin is completely hydrolyzed, the diaqua nedaplatin form approaches

DNA [2, 26]. With these steps a charged active drug is generated and then it can further interact with the nucleophilic part of DNA. In reaction path 1, as a result of the addition of one water molecule to the drug, nedaplatin's ring is opened and A is obtained. With the addition of a second water molecule to A in reaction path 2, molecule B and ligand C products are obtained with the SN^2 mechanism.

In reaction paths 3 and 4, cysteine reactions occur with B. As can be seen from the fukui indices values of nedaplatin and cysteine listed in Table 3, S and N atoms of cysteine are suitable sites for the reaction. Therefore, the interactions of cysteine and nedaplatin with the S and N atoms were investigated in paths 3 and 4. It is also stated in the literature that diaquanedaplatin (B) interacts with the S atom of cysteine and the N atoms of amino acids [4]. Thus, our result coincides with the literature. In path 3, the interaction of cysteine and B atom with S atom led to the formation of the monodentate cysteine complex (D). Finally, the bidention D molecule is formed from the N atom of cysteine and the Pt atomic part of nedaplatin. then E molecule is obtained by separating a water molecule. The molecular structures of the reaction intermediate for path 3 are given in Fig. 4. The molecular structures for other paths are given in the Supplementary information.

CONCLUSION

In this study, the electronic properties of cisplatin, carboplatin, oxaliplatin, nedaplatin, lobaplatin, and heptaplatin were investigated by the DFT method. Reactivities of the drugs were calculated by the means of global reactivity indices. Global reactivity indices results demonstrate that cisplatin is the most reactive molecule. The reaction of nedaplatin with cysteine amino acid was also analyzed by using local indices. For the molecules studied, Pt atoms according to the fukui indices values, as with nedaplatin, are suitable sites that can react with the nucleophilic region of the DNA molecule. In general, in platinum-containing drugs, as understood from the fukui indices, the Pt atom is the region that can react with amino acids. This study provides a theoretical basis for predicting the electronic properties of Pt-containing anticancer drugs and their reactivity.

Acknowledgement: *The authors of this study declare that there is no financial support for this study.*

REFERENCES

1. Y. Arbia, S. Abtouche, M. Dahmane, M. Brahimi, *Theor. Chem. Acc.*, **142**(1), (2023).
2. M.E. Alberto, V. Butera,N. Russo, *Inorg. Chem.* **50**(15), 6965 (2011).
3. ACPt 14) M1 rosenberg1969, (n.d.).
4. T. Minervini, B. Cardey, S. Foley, C. Ramseyer, M. Enescu, *Metallomics*, **11**(4), 833 (2019).
5. M. Torres, S. Khan, M. Duplanty, H.C. Lozano, T.J. Morris, T. Nguyen, Y. V. Rostovtsev, N.J. Deyonker, N. Mirsaleh-Kohan, *Journal of Physical Chemistry A*, **122**(34), 6934 (2018).
6. A. de Almeida, R. Bonsignore, *Bioorg. Med. Chem. Lett.*, **30**(13), (2020).
7. A. Pöthig, A. Casini, *Theranostics*, **9**(11), 3150 (2019).
8. C.A. Rabik, M.E. Dolan, *Cancer Treat. Rev.*, **33**(1), 9 (2007).
9. D. Miodragović, A. Merlino, E.P. Swindell, A. Bogachkov, R.W. Ahn, S. Abuhadba, G. Ferraro, T. Marzo, A.P. Mazar, L. Messori, T. V. O'Halloran, *J. Am. Chem. Soc.*, **141**(16), 6453 (2019).
10. L. Qi, Q. Luo, Y. Zhang, F. Jia, Y. Zhao, F. Wang, *Chem. Res. Toxicol.*, **32**(8), 1469 (2019).
11. S.H. Chen, J.Y. Chang, *Int. J. Mol. Sci.*, **20**(17), (2019).
12. E. Shakerzadeh, *Comput. Theor. Chem.*, **1202**, (2021).
13. J. Zhang, T. Zhao, C. Wang, Q. Meng, X. Huo, C. Wang, P. Sun, H. Sun, X. Ma, J. Wu, K. Liu, *Oxid. Med. Cell Longev.*, **2021**, (2021).
14. N.M.D. Sandhiutami, W. Arozal, M. Louisa, D. Rahmat, P.E. Wuyung, *Front. Pharmacol.*, **11**, (2021).
15. A.A. Piya, S.U.D. Shamim, M.N. Uddin, K.N. Munny, A. Alam, M.K. Hossain, F. Ahmed, *Comput. Theor. Chem.*, **1200**, (2021).
16. M. Salihović, M. Pazalja, S. Špirtović Halilović, E. Veljović, I. Mahmutović-Dizdarević, S. Roca, I. Novaković, S. Trifunović, *J. Mol. Struct.*, **1241**, (2021).
17. Gaussian 09, Revision B.04, Gaussian Inc., Pittsburgh, PA, 2009.
18. R. Dennington, T. Keith, J. Millam, GaussView, Version 5, Semichem Inc., Shawnee Mission, KS, 2009.
19. J. B. Foresman, A. Frisch, Exploring Chemistry with Electronic Structure Methods, Gaussian Inc., USA,1996.
20. Y.Y. Gurkan, N. Turkten, A. Hatipoglu, Z. Cinar, *Chemical Engineering Journal* **184**, 113 (2012).
21. W. Yang, R.G. Parr, *Proc. Natl. Acad. Sci. USA*, **82**, 6723, (1985).
22. R.G. Parr, W. Yang, Density Functional Theory of Atoms and Molecules, Oxford Univ. Press, New York, 1989.
23. R.K. Roy, S. Pal, K. Hirao, *Journal of Chemıcal Physıcs*, **110** (17), 8236 (1999).
24. M. Malik, D. Michalska, *Spectrochim Acta A, Mol. Biomol. Spectrosc.*, **125**, 431 (2014).

25. G.H.W. Milburn, M.R. Truter, *Journal of the Chemical Society A: Inorganic, Physical, Theoretical*, 1609 (1966).
26. M.E. Alberto, M.F.A. Lucas, M. Pavelka, N. Russo, *Journal of Physical Chemistry B* **113**(43), 14473 (2009).
27. R.G. Pearson, Chemical Hardness and Density Functional Theory, 2005.
28. L.R. Domingo, P. Pérez, *Org. Biomo.l Chem.*, **9**(20), 7168 (2011).
29. M. Elango, R. Parthasarathi, G. K. Narayanan, A.M. Sabeelullah, U. Sarkar, N.S. Venkatasubramaniyan, V. Subramanian, P.K. Chattaraj, *Journal of Chemical Sciences*, **117,** 61 (2005)
30. S. Aydogdu, A. Hatipoglu, *Acta Chim. Slov.*, **69**(3), 647 (2022).
31. I. Erden, A. Hatipoglu, C. Cebeci, S. Aydogdu, *J. Mol. Struct.*, **1201**, (2020).
32. D. Corinti, R. Paciotti, C. Coletti, N. Re, B. Chiavarino, M.E. Crestoni, S. Fornarini, *J. Inorg. Biochem.*, **237**, (2022).
33. T. Zimmermann, M. Zeizinger, J. V. Burda, *J. Inorg. Biochem.*, **99**(11), 2184 (2005).